

# **Diffusion-limited characteristics of mechanically induced current in polypyrrole/Au-membrane composite**

Wataru Takashima<sup>1)\*</sup>, Shunsuke Kawamura<sup>2)</sup>, and Keiichi Kaneto<sup>2)</sup>

<sup>1)</sup>*Research Center for Advanced Eco-fitting Technology,*

<sup>2)</sup>*Graduate School of Life Science and Systems Engineering,*

*Kyushu Institute of Technology,*

*2-4 Hibikino, Wakamatsu, Kitakyushu, Fukuoka 808-0196, Japan*

\*(corresponding author)

e-mail:watakashi@lsse.kyutech.ac.jp

Tel/fax:+81-93-695-6049

© 2011. This manuscript version is made available under the CC-BY-NC-ND 4.0 license <http://creativecommons.org/licenses/by-nc-nd/4.0/>

## **Abstract:**

Mechanically induced current (MIC) was investigated in a polypyrrole/Au-coated membrane (PPy/Au-membrane) composite with various surface morphologies as well as electrolyte conditions in electrochemical cell. MIC was obtained in porous PPy/Au-membranes with thin PPy deposition. Against this, relative small MIC was observed in non-highly porous films such as freestanding films as well as PPy/Au-membranes with thick PPy deposition. One order small MIC was also observed in an Au-membrane without PPy. These results indicate that MIC is a charging phenomenon to both the redox and the double layer capacitances. MIC also varies with supporting electrolyte as well as its concentration. MIC is strongly reduced in solutions with diluted electrolyte and with bulky cation electrolytes, indicating that the number and the penetration speed of mobile ion limit MIC magnitude. These finding characteristics represent that MIC is essentially diffusion limited current. A two-electrode MIC cell was also configured to investigate as a power generation film in normal saline solution possibly utilizing for biomedical application.

Keywords: mechanically induced current; electrochemical; polypyrrole; soft actuator; diffusion

## 1. Introduction

A mechanically induced current (MIC) in an electrochemical soft actuator is an interesting function that provides a strain sensor [1] and a power generation film. This functionality, combined with other features on soft actuators, such as light weight nature, flexibility and biocompatibility, [2] can provide the possibility of fabrication novel-type sensors and related devices. Recently, both the MIC and the electrochemo-mechanical deformation (ECMD) have been frequently reported by many researchers. [3, 4] These facts have suggested that redox active materials can convert between the energy states (i.e., electrochemical and mechanical states). Thus, a MIC is a type of counter-phenomenon of ECMD for redox active film. [5] Further investigations of MICs have provided structural optimization and modeling of coupling parameters between electrochemical and mechanical energies, and have been recently reported by several groups.[6, 7]

Charging an electronic double layer could be another route utilized for generating a MIC. A blank measurement would be required to investigate the individual contribution of the electronic double layer or the redox components. The mixing characteristics of both the electronic double layer and the redox components have already been reported by analyzing the cyclic voltammetry (CV) data for conducting polymers. [8-10] The physical charging values caused by a change in area, as in the electronic double layer, can be identified by the current level involved in the MIC. Similarities between the dependence of the MIC on the size of the ion or its concentration in the electrolyte should be investigated and compared to the redox contribution of the electrochemical actuator previously reported. [11, 12] These

characteristics could lead to the mechanism and a way to enhance the MIC effect.

The fabrication of these sensitive devices has provided a detailed insight of the generation mechanism for MICs and possible applications for practical use. Surface porosity has been determined to be a key factor for improving the redox current. A similar concept has also been incorporated to increase the actuation performance. [13] Incorporating a membrane filter into the device can be another route to fabricate the porous actuation films for supporting its freestanding characteristics, even with a thin active film deposition. Au possesses high ductility; therefore placing a Au coating on the filter surface before depositing the polymer can be an effective method to provide metallic high-conductance, even under expansion, by which the whole film surface can be held at the same redox potential. Thus the device can become sensitive to the redox equilibrium because of the highly conducting network by the Au.

A two-electrode structure has been determined to be an important configuration for the practical use of an electrochemical device. A two-electrode type MIC film can be fabricated even with a single type PPy or complemented ion exchange PPy films. A two-electrode MIC film can be utilized as a power source film. The biocompatibility of polymers could incorporate such devices as power sources into human bodies with low-impact.

Herein, MIC with ECMD in PPy freestanding films and Au-coated membrane (Au-membrane) composites with or without PPy deposition were investigated. MIC characteristics were investigated in PPy/Au-membrane composites as functions of the

thickness of PPy, type of electrolyte and electrolyte concentration. The change in the magnitude of MICs in terms of the diffusive characteristics of the mobile ion with ECMD behaviors was also discussed. A two-electrode MIC device was also fabricated to investigate the output characteristics and the MIC generation functionality in buffer saline solution for practical use.

## **2. Experimental**

The basic experimental conditions can be found in the literature. [14] The pyrrole monomer was distilled, and the other chemicals were used as received. The normal saline solution (NSS) was purchased from Otsuka Pharmaceutical Co., Ltd. The electrodeposition was performed in a dodecylbenzene sulfonate (DBS) solution galvanostatically at 1.0 mA/cm<sup>2</sup> at a range of times points to vary the concentration of the PPy coating. The ECMD, CV and MIC measurements were obtained using samples with the same rectangular shape in a single compartment of an electrochemical cell as previously reported (Fig.1). [14] The MIC was generated by modulating the load of 1.0 MPa under the application of a base load of 0.1 MPa. The supporting electrolyte was dissolved in degassed distilled water at the standard concentration of 1.0 M unless otherwise noted.

[Figure 1]

## **3. Results and Discussion**

### **3.1 Contribution of the Electronic Double Layer on the MIC.**

[Figure 2]

Figure 2 shows the induced current vs. electrochemical potential applied on an Au-membrane film without the PPy deposition. The figure illustrates that a MIC can be generated without PPy. The MIC potential map shows a proportional increase as a function of the absolute potential vs. polarity switch around the zero-potential region. These features are unlike those found in literature, [5, 14] which indicated that the MIC observed herein was attributed to the (dis)charging of the electronic double-layer capacitor with the modulation of the surface area caused by the tensioning load. However, the current level of this MIC was approximately one order of magnitude smaller than that in the PPy/Au-membrane composite described later in this document. Although the double layer charge was involved to some extent, the latter suggested that the MIC was dominated by the redox component. The dual components of the redox and the double layer charges have been already confirmed via electrochemical studies of conducting polymers. [8-10] It was important to note the duality between the charging behaviors in the MIC and the redox characteristics as it revealed the correlation between the MIC and ECMD via the electrochemistry of conducting polymers.

### **3.2 Surface Morphology Effect.**

[Figure 3]

The contribution of the surface porosity on the MIC was investigated in the

PPy/Au-membrane and in the freestanding PPy films. The electrodeposition of PPy was tuned to control the weight per area of PPy to be  $0.9 \text{ mg/cm}^2$  for both the PPy/Au-membrane and PPy freestanding films. Figure 3 shows the potential map of the MIC, ECMD and the CV characteristics with the same load modulation. The composite film induced a larger MIC across the entire potential region. The largest MIC was obtained at the cathodic potential regions for both films, indicating that the intrinsic MIC characteristics were essentially similar. Little difference was found in the peak potential region of the MIC that corresponded to the difference of the ECMD and the CV peaks in Fig.3 (b). The maximum strain of ECMD was 1.2% in the composite film, which was a little small as compared to that in the freestanding film of 1.4 %.

The decrease in the ECMD for the composite was attributed to the increase in the film modulus. The mechanical support of the Au-membrane hindered the free motion of PPy by the addition of the film modulus. The change in length of the film between the loading and releasing of the load was approximately 1.5 mm for PPy/Au-membranes, which was slightly shorter than the 1.7 mm for PPy freestanding films; this represented an increase in the film modulus with incorporation of the membrane. The decrease of the ECMD in the PPy/Au-membrane composite also corresponded to the decrease of the ECMD in mechanically pre-stretched films in a uniaxial direction to the stroke as reported for PPy [15] and for polyaniline [16] films; this was also to increase the self-modulus by mechanical stretch.

The CV curves in Fig.3 (b) also show a narrow potential peak that corresponds to

the small hysteresis of the ECMD on electrochemical potential. These features represented the sensitive response of the composite film to the application of the external stimuli in both the redox potential and the load application. An electrode coated with Au contributed to uniformly applying the redox potential over the entire composite film, which contributed to effectively relay the MIC to the electrode.

The freestanding PPy possessed a small Young modulus and a large ECMD compared to their corresponding values in the PPy/Au-membrane composite. Conversely, a large MIC was obtained in the PPy/Au-membrane. These findings indicated that the large ECMD and/or the small modulus were not indispensable requirements for a large MIC. The surface porosity dominated for the effective MIC generation. The peak current of the MIC was consistently evaluated to compare the magnitude of the MIC in this study. In addition, the total charge integrated with the MIC is an important parameter for discussion. A detailed investigation for the relationship between the MIC and ECMD related to the film modulus should be performed on the freestanding PPy films, as the PPy/Au-membrane composites is a unique film.

[Figure 4]

Figure 4 (a) shows a comparison of the MIC polarized at  $-300\text{mV}$  in PPy/Au-membrane composites with various PPy deposition times. The spike-wise MIC was reproducibly appeared by applying and releasing a load for all of the films. Comparing the responses of the MIC for these three films (in Fig. 4(b)), the decay time ( $\tau$ ) of the MIC

clearly increased with the deposition time at this polarization condition. These features indicated that the MIC was generated by the diffusion of the mobile ions.

[Figure 5]

Figure 5 shows the SEM micrographs of the film surface. A short-time deposition was found to preserve the fine surface porosity of the Au-membrane. The changes in surface porosity found with the deposition times shown in Fig. 5 corresponded well with the characteristics of the MIC. The diffusion limit characteristics of the MIC revealed here were the same of those in the redox current of conducting polymers as commonly reported.

[Figure 6]

Figure 6 shows ECMD, CV and the potential dependence of the MIC observed in the composite films shown in Fig. 4. The CV data correlated well to the amount of PPy deposited on the Au-membrane. The ECMD also increased with PPy deposition. A large shrink force in the thick PPy/Au-membrane caused an increase in the ECMD magnitude. The thin PPy/Au-membrane composite also generated a MIC over the entire potential region.

The magnitude of the MIC ( $j_{MIC}$ ) observed in a diluted solution can be represented as the diffusion current proportional to the concentration of the mobile ion ( $C$ ) in the film and the modulated load applied to the film ( $\Delta p$ ) as a single ion exchange model; this can be used as the first coarse approximation, which is already discussed in the literature. [14]

$$j_{\text{MIC}} = kC\Delta p \quad (\text{a})$$

Thus, the concentration of the mobile ion in the film is, was considered to be one of the main factors for the MIC.

The composite film with the thick PPy coating dominated the large MIC at the narrow cathodic region, which was attributed to the total amount of mobile cation ( $\text{Na}^+$ ) that increased with thicker PPy. The MIC, however, diminished at the anodic region. This was probably due to the essential decrease of the number of mobile cations at this potential region. The modulation of the surface area with the load application might have not generated much cationic diffusion due to a small population with small porosity of the film surface in this state. In addition, the thick PPy generated the potential distribution due to the IR drop along with the thickness, which limited the MIC activity with  $\text{Na}^+$  population. These findings indicate that the thick PPy composite strongly characterized the MIC by the doping state. Conversely, the thin PPy composite was effective at sensing the MIC over the wide potential region, which could have been because of a small IR drop in the thickness.

### **3.3 Electrolyte Effect.**

[Figure 7]

Figure 7 shows the induced current dependence on the concentration of the supporting electrolyte. The current seemed to increase with increasing the concentration except at the

highest electrolyte concentration of 3M NaCl/aq.

The cation exchange with PPy can be represented by the following redox equilibrium equation:



Substituting these values in the Nernst equation provides the electrochemical potential represented as follows:

$$E = E_0 + \frac{k_B T}{zF} \ln \left( \frac{[\text{PPyDBS}^-][\text{Na}^+]}{[\text{PPyDBS}^- \text{Na}^+]}\right) = E_0 + \frac{k_B T}{zF} \ln([\text{Na}^+]) \quad (\text{b})$$

where  $k_B$ ,  $T$ ,  $z$  and  $F$  denote the Boltzmann constant, absolute temperature, valence of the reaction and Faraday constant, respectively. Although this was one of the possible reasons for the non-linear relation shown in Fig.7 that was caused by the shift of electrochemical potential by the dilution of electrolyte, another explanation was required for the decrease of the MIC at high electrolyte concentration.

The electrochemical equilibrium of the mobile ion can be represented as the balance of the difference of Gibbs free energy with the electrochemical potential of mobile ion between the inside and the outside of the film. Therefore, the redox potential towards the cathodic polarity was used to pump cations into the film in a condensed state, by which the mobile ion obtained high electrochemical potential. This effect was valid for the

electrochemical equilibrium in a relatively dilute system. The highly concentrated system, however, possibly failed to identify the electrochemical potential only by a single ion equilibrium level, as represented in eq. (2). [17] The same concentration dependence is shown in Fig. 7 and has already been reported for the ECMD of PPy films in the literature. [11, 18]

PPy is known to be fully doped at 33% of the monomer-unit. [19] This suggested that the concentration of mobile ion at fully injected state in the film was estimated to be around 2.5 M when the density of PPyDBS was approximately  $1.2\text{g/cm}^3$  [20] and fully doped by  $\text{DBS}^-$ . This value is regarded as the maximum concentration needed to condense a single ion in PPy by electrochemical potential. The decrease of both the MIC and the ECMD when approaching this concentration limit could be caused by the saturation of the ion concentration both inside and outside of PPy. The osmotic contribution, could possible explain the decrease of the ECMD in this condensed state. [17] Anion exchange was coincidentally generated to balance the redox charge, which possibly reduced both the MIC and the ECMD due to the compensation effect of the simultaneous anion and cation exchange. [11, 21]

[Figure 8]

Cation dependence on the induced current was also investigated. Figure 8 (a) shows a cation dependence of the MIC and the diffusion coefficient ( $D$ ) estimated by step-pulse voltammetry as a coarse approximation with the following equation:

$$f = \frac{4\sqrt{D}}{d\sqrt{\pi}}\sqrt{t} \quad (3)$$

where,  $f$  and  $d$  denote the normalized charge and film thickness, respectively. [22] This calculation involved some errors, particularly in the thickness of the electro-active film in the PPy/Au-membrane composite. The film thickness depended on one factor, therefore, a comparison of the difference of diffusion coefficient could be discussed with the values obtained in this analysis. Supporting electrolytes of all the alkaline metal chloride salts provided relatively large values for the MIC. In case of the alkylammonium chloride salts, except ammonium, the MIC was quite small although the polarity of the MIC was conserved in the same manner.  $D$  was strongly decreased within 1.5 orders of magnitude for large alkylammonium salts. This relationship clarified that the diffusion speed of the cation in PPyDBS determined the magnitude of the MIC.

A large MIC appeared in the electrolytes having small cations. A maximum current was observed with the Li electrolyte; which was controversial when compared to the large ECMD value because of the large Stokes radii with solvation, [23] which possibly reduced the diffusion speed. The magnitude of the ECMD was not simply correlated to the magnitude of the MIC. The cation was well solvated with several water molecules. [24] A large electrochemical creep also appeared for the *p*-phenolsulfonate doped PPy when the redox-cycle began in the aqueous LiCl solution. [25] These results indicated that the swelling state of the PPy by water under reduction (cation incorporation) improved the solvated cation transport. [23] Both the electrochemical creep and the MIC are considered a

transient phenomenon with ion flux. [25, 26] Conversely, the ECMD was a quasi-static phenomenon. A collective total charge for the MIC could be correlated to the ECMD. A comparison of the MIC with the speed of the ECMD could disclose their relationship more precisely.

The relationship between  $D$  and MIC is illustrated in Fig. 8 (b). This figure clarified that both the MIC and  $D$  were distributed in the same dynamic range of approximately 1.5 orders, although they exhibited a large variation. Three univalent alkali metal cations were almost linearly correlated to  $D$ , while alkyl ammonium cations were ruled out. The difference in solvation structure of these cations [23] was used to categorize the plots in these two groups. The MIC exhibited a monotonic increase as a function of  $D$  for all cations.

It should be noted that we have tried to investigate the anion dependence of MIC by using anion exchange PPy electrodeposited in TFSI salts.[14] This PPyTFSI, however, almost failed to show clear relationship with various electrolytes, such as  $\text{NaClO}_4$ ,  $\text{NaBF}_4$ ,  $\text{NaPF}_6$ ,  $\text{NaBr}$ ,  $\text{NaCl}$ ,  $\text{NaI}$  and  $\text{NaF}$ . This means that anion exchange in PPy is a little difficult to clarify the anion dependence unlike the cation exchange.[25] It may be attributed to the difference of the contribution of anion or cation exchange for PPy. Although anion being the right counter ion for the oxidation of PPy, cation is simply exchanged as the charge compensation with electrochemical charge equilibrium.

As another explanation,  $\text{DBS}^-$  being well stranded in PPy, the initial dopant will

provide free-volume in PPy as a plasticizing dopant,[4,27] by which the diffusion path for cation is conserved with the stable viscoelasticity of PPyDBS. Therefore, the cation exchange contribution in PPy possibly supports to display the diffusive characteristics. On the contrary, the anion exchange PPy basically switches from the doped state at oxidation potential to the non-doped (ionic empty) state at reduction potential. In this case, the PPy film tends to show a relative large ECMD by a pure contribution to expand the film with a little slow response[28] possibly accompanied by the change in the film elasticity due to the plasticizing dopant removal.

### **3.4 Two-electrode Configuration as Power Generation Films**

A freestanding two-layer device was fabricated and evaluated in the output performance. The anodic layer was consisted of a PPy(TFSI)/Au-membrane composite as anion exchange layer, while the cathodic layer was consisted of a PPy(DBS)/Au-membrane one as cation exchange layer, respectively. This device, therefore, operates as a linear actuator. Therefore, loading with a weight on the two-electrode device provides PPy(TFSI)/Au-membrane as anion injection and PPy(DBS)/Au-membrane as cation injection coincidentally, by which current can circulate with the same deformation stimuli.

The redox activity of the two-electrode device was investigated at various electrochemical potentials initialized by the following procedure:

- 1) shorted two electrodes of the two-layer device in order to dope both PPy layers into the same redox level

2) configured a three electrode electrochemical cell with the shorted two-electrodes as one working electrode, a Ag/AgCl wire as reference electrode, and a Pt as counter electrode, respectively.

3) hold the working electrode at various electrochemical potentials to initialize the doping states of the two-electrodes in the same redox level.

4) re-configured the two-electrode device into the setup as shown in Fig.9 (a) followed to operate CV and ECMD.

[Figure 9]

Figure 9 (b) shows CV curves of the two-electrode device as two-electrode electrochemical cell configuration. This figure indicates that the redox activity of the two-electrode device was strongly influenced by the initialization potential. Figure 9 (c) shows the redox charge as a function of the initialization potential. A peak potential of -700mV was found as the best initialization potential to form the highest electrochemical activity-state in the two-electrode device in this results. As-deposited PPy being a fully doped state, for configuring an active two-electrode device, both of the PPy layers should be initialized as an intermediate state, by which both the PPy layers can operate toward both oxidized and reduced states, respectively.

[Figure 10]

Figure 10 (a) shows MIC as a function of the bias applied between the anode and

the cathode of the two-electrode device in 1.0M NaCl/aq. solution. This figure is almost corresponding to the output characteristics of Solar-cell. Appearance of a maximum current at around 400mV in this figure might be attributed to still not enough of the fine tuning of the electrochemical potential for initialization. The result indicates that the two-electrode device can generate the persistent MIC in the same sign even under applying external bias of 1.5 V. This is a little high voltage beyond the expectation, which probably represents the MIC characteristics caused by not the electrochemical process but the diffusive generation of mobile ion by mechanical stimuli. This characteristic is possible to utilize the device to the practical use. Replots of Fig.10 as output power per weight of PPy provide the possible power to generate in this film to be several  $\mu\text{W}/\text{mg}$ .

[Figure 11]

MIC generation in two-electrode device was also operated in a normal saline solution (NSS) without biasing. Figure 11 shows that MIC can be generated even in NSS although the sign of MIC is a little complicated. In this case, the electrochemical potentials of both the electrodes are identified with the doping state by equilibrating the mobile ions of both the PPy/Au-membranes. Unbalance of diffusion speed of various mobile ions in each PPy layer will cause such overshoot characteristics in MIC. The finding persistent generation of MIC in NSS indicates that the two-electrode device is possibly utilized as a miniature power source film incorporative in life-beings' body. Increasing the film area with multifold structure can easily increase the output power, by which a C-MOS circuit to stimulate retina cells is possibly operated for instance. The eyes blinking may use to

generate small MIC current to drive the C-MOS for visualizing images by this power film for the visually impaired whenever he wants.

#### **4. Conclusions**

In this report, we demonstrated the mechanically induced electrochemical current (MIC) in cation exchanged composite membrane film on which Au and electrodeposited polypyrrole in dodecylbenzenesulfonic acid (PPyDBS). Component of the electronic double layer charging in MIC was revealed. Morphological effect of the film surface on MIC was also investigated for the improvement of MIC. Diffusion limited characteristics of MIC were revealed with film morphology, electrolyte concentration and electrolyte dependence.

Two-electrode cell was configured to investigate as a power source film. The output voltage can over 1.5 V with 4  $\mu$ A as the maximum MIC was obtained. The device was found to generate MIC even in normal saline solution, which demonstration will show the possible use of MIC as a miniature power-source film incorporative to the life-being.

#### **Acknowledgements**

This study was financially supported by Mazda Foundation and by a Grant-in-Aid for Scientific Research in the Priority Area (B) (No.21350103) from Japan Society for the Promotion of Science.

## Figure captions

Figure 1: Electrochemical cell configuration with measurement system set-up and chemicals

Figure 2: Potential dependence of MIC in Au-membrane film. Solid circles and open circles represent MICs with applying and releasing a 1 MPa load, respectively.

Figure 3: Comparisons of (a) Potential dependence of MIC under applying (solid symbols) and releasing (open symbols) and (b) CV (upper panel) and ECMD (lower panel) characteristics. Dotted lines represent in a freestanding film and solid lines in a PPy/Au-membrane composite, respectively.

Figure 4: MIC responses polarized at  $-300$  mV vs. Ag/AgCl in PPy/Au-membrane composites electrodeposited for various times.

Figure 5: SEM micrographs of (a) a freestanding PPy film, PPy/Au-membrane composites electrodeposited for (b) 500 s, (c) 1500 s and (d) 4500 s, respectively.

Figure 6: (a) Potential dependence of MIC and (b) ECMD and CV curves, in PPy/Au-membrane composites deposited for 500s (solid line), 1500s (dashed line) and 4500s (dotted line), respectively.

Figure 7: NaCl concentration dependence of MIC polarized at  $-600$ mV vs. Ag/AgCl.

Figure 8: (a) Cation dependence of MIC (upper panel) and diffusion coefficient ( $D$ ) (lower panel) measured with step-pulse voltammetry polarized at  $-600\text{mV}$  vs. Ag/AgCl. (b) Relationship between  $D$  and MIC obtained by applying (solid circle) and releasing (open circle) a  $1\text{ MPa}$  load on the film.

Figure 9: (a) Configuration set-up of the MIC measurement using the two-electrode device, (b) CV curves of the two-electrode device initialized at various electrochemical potentials, and (c) redox charges estimated with CV curves as a function of the initialized electrochemical potential.

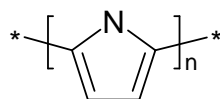
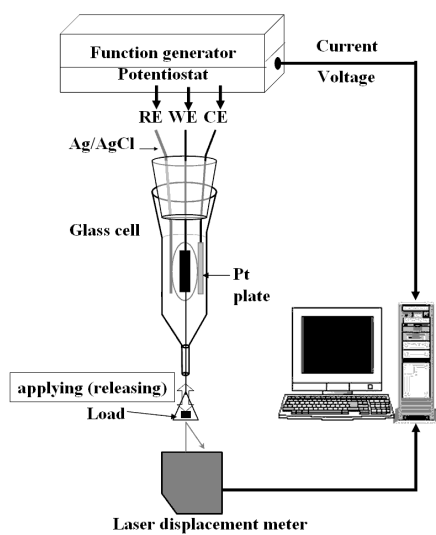
Figure 10: (a) External bias dependence of MIC generated applying (solid circle) and releasing (open circle) a  $1.0\text{ MPa}$  load in a two-electrode device and (b) estimated output power as a function of external bias.

Figure 11: A response of MIC in a two-electrode device in NSS solution.

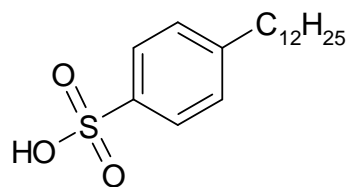
## References

- [ 1] Y. Wu, G. Alici, J.D.W. Madden, G.M. Spinks, G.G. Wallace, *Adv. Func. Mater.* 17 (2007) 3216.
- [ 2] E. Smela, *Adv. Mater.* 15 (2003) 481.
- [ 3] L.V. Conzuelo, J. A.-Pardilla, J.V. C.-Rodríguez, M.A. Smit, T.F. Otero, *Sensors.* 10 (2010) 2638.
- [ 4] K. Kaneto, H. Suemasu, K. Yamato, *Bioinsp. Biomim.* 3 (2008) 035005.
- [ 5] W. Takashima, T. Uesugi, M. Fukui, K. Kaneto, *Synth. Met.* 85 (1997) 1395.
- [ 6] S.W. John, G. Alici, G.M. Spinks, J.D. Madden, G.G. Wallace, *Smart. Mater. Struct.* 18 (2009) 085007.
- [ 7] T. Shoa, J.W. Madden, T. Mirfakhrai, G. Alici, G.M. Spinks, G.G. Wallace, *Sens. Actuators. A.* 161 (2010) 127.
- [ 8] J. Tanguy, N. Mermilliod, M. Hoclet, *Synth. Met.* 18 (1987) 7.
- [ 9] M. Grzeszczuk, P. Poks, *J. Electrochem. Soc.* 146 (1999) 642.
- [10] S.L.G. Lissy, S. Pitchumani, K. Jayakumar, *Mater. Chem. Phys.* 76 (2002) 143.
- [11] W. Takashima, S.S. Pandey, K. Kaneto, *Thin. Solid. Films.* 438 (2003) 339.
- [12] Y. Kato, K. Tada, M. Onoda, *Jpn. J. Appl. Phys.* 42 (2003) 1458.
- [13] L. Bay, K. West, S. Skaarup, *Polymer.* 43 (2002) 3527.
- [14] W. Takashima, K. Hayashi, K. Kaneto, *Electrochem. Commun.* 9 (2007) 2056.
- [15] R.Z. Pytel, E.L. Thomas, I.W. Hunter, *Chem. Mater.* 18 (2006) .
- [16] W. Takashima, M. Fukui, M. Kaneko, K. Kaneto, *Jpn. J. Appl. Phys.* 34 (1995) 3786.
- [17] L. Bay, T. Jacobsen, S. Skaarup, K. West, *J. Phys. Chem. B.* 105 (2001) 8492.

- [18] K. Kaneto, Y. Sonoda, W. Takashima, *Jpn. J. Appl. Phys.* 39 (2000) 5918.
- [19] V.P. Menon, J. Lei, C.R. Martin, *Chem. Mater.* 8 (1996) 2382.
- [20] J.Y. Lee, D.Y. Kim, C.Y. Kim, *Synth. Met.* 74 (1995) 103.
- [21] S. Skaarup, L. Bay, K. Vidanapathirana, S. Thybo, P. Tofte, K. West, *Solid. State. Ionics.* 159 (2003) 143.
- [22] K. Kaneto, M. Kaneko, W. Takashima, *Jpn. J. Appl. Phys.* 34 (1995) L837.
- [23] W. Takashima, H. Hashimoto, K. Tominaga, A. Tanaka, S.S. Pandey, K. Kaneto, *Thin Solid Films* 519 (2010) 1093.
- [24] K.P. Vidanapathirana, M.A. Careem, S. Skaarup, K. West, *Solid. State. Ionics.* 154-155 (2002) 331.
- [25] W. Takashima, S.S. Pandey, M. Fuchiwaki, K. Kaneto, *Jpn. J. Appl. Phys.* 41 (2002) 7532.
- [26] Q. Pei, Olle Inganäs, *J. Phys. Chem.* 96 (1992) 10507.
- [27] B. Dufour, P. Rannou, D. Djurado, M. Zagorska, I. Kulszewicz-Bjer, A. Pron, *Synth. Met.* 135 (2003) 63.
- [28] S. Hara, T. Zama, W. Takashima, K. Kaneto, *J. Mater. Chem.* 14 (2004) 1516.



polypyrrole



dodecylbenzene sulfonate

Figure 1: W. Takashima

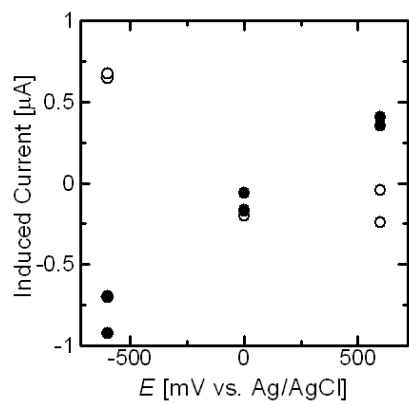


Figure 2: W. Takashima

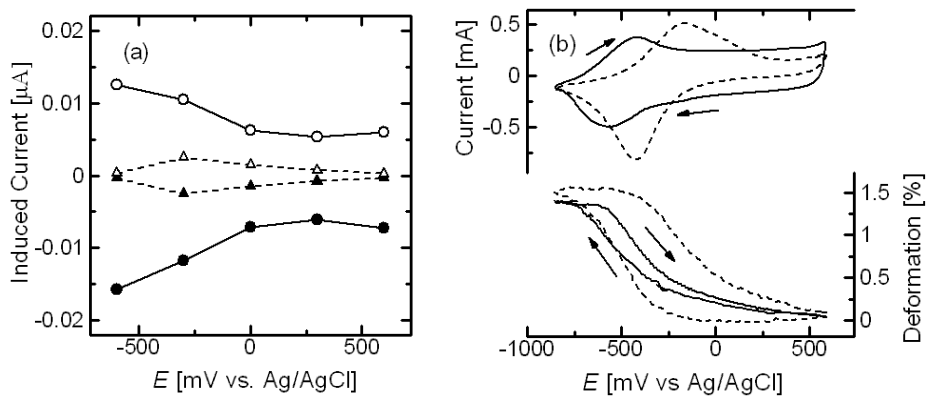


Figure 3: W. Takashima

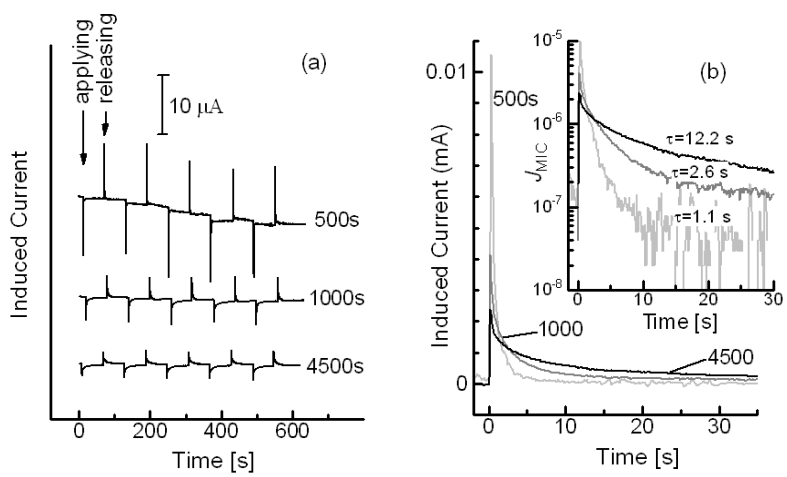


Figure 4: W. Takashima

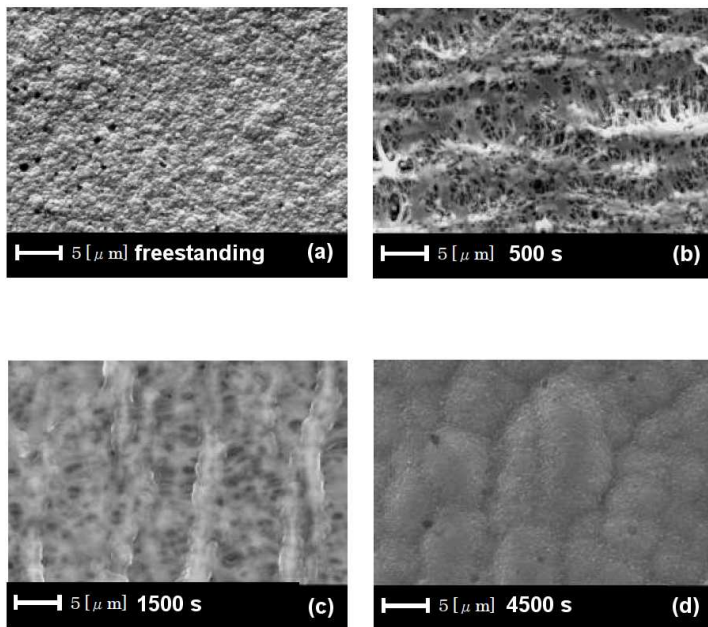


Figure 5: W. Takashima

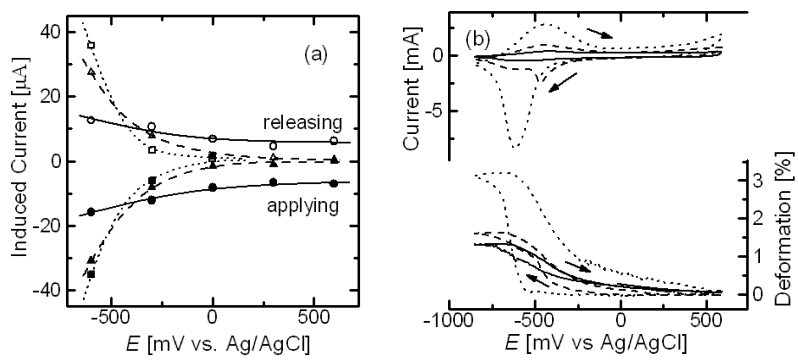


Figure 6: W. Takashima

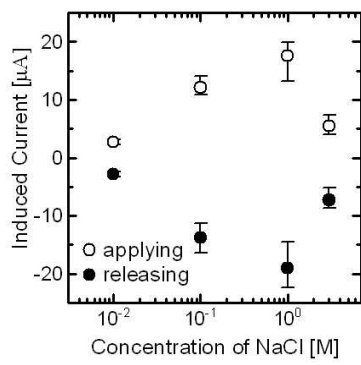


Figure 7: W. Takashima

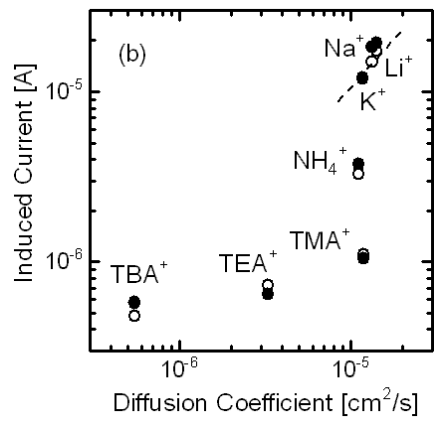
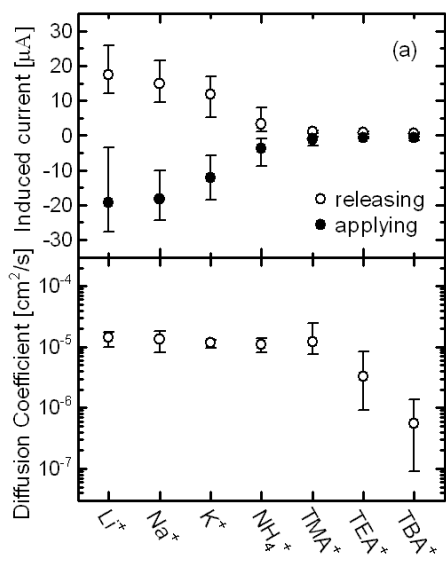


Figure 8: W. Takashima

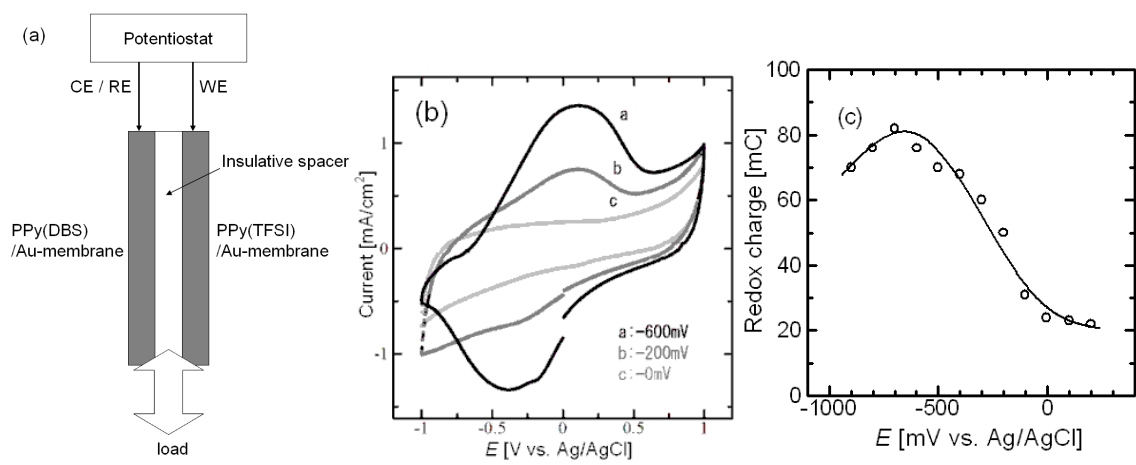


Figure 9: W. Takashima

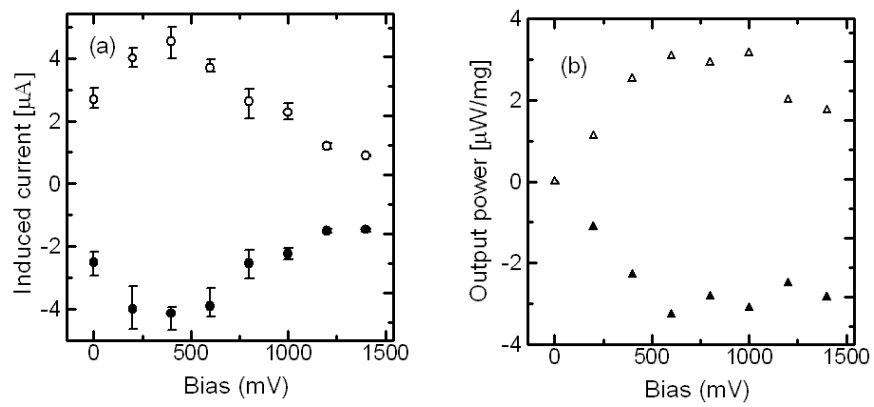


Figure 10: W. Takashima

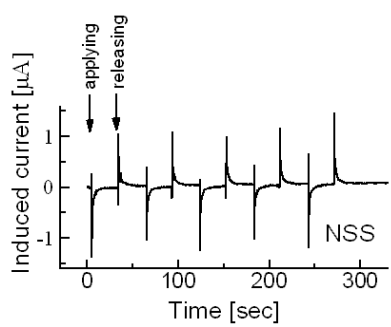


Figure 11: W. Takashima